

An initial look at modelling echo from an air hose during the Target and Reverberation Experiment 2013

Dale D. Ellis¹ and Jie Yang²

¹Department of Physics, Mount Allison University, Sackville, NB, Canada

²Applied Physics Laboratory, University of Washington, Seattle, WA, USA

Contact: Dale D. Ellis, 18 Hugh Allen Drive, Dartmouth, NS, Canada B2W 2K8

email: daledellis@gmail.com

Abstract: *The Target and Reverberation Experiment (TREX13) was conducted in shallow water (~ 20 m water depth) in the Gulf of Mexico off Panama City, Florida, USA. Extensive acoustic measurements were made in April and May 2013 using LFM pulses in various sub-bands between 1800 and 3600 Hz, generally with both source and receiver in fixed-fixed position. Previous work has concentrated on reverberation characteristics at the site. In this work the focus is on modelling the echo return from a vertically deployed 15-m air-filled hose. The primary receiver was the FORA triplet array deployed horizontally in near-monostatic geometry. Here a normal mode based approach is adopted to predict the echo returns. A complete model would consider the coherent scattered field as a function of depth along the array at multiple frequencies, and convolve with a pulse propagation model to compare with the processed (pulse-compressed) data. A simpler approach using an energy-based model at a single frequency with modal group velocities is utilized to synthesize the received echo. Various scattering models are discussed: an omnidirectional point scatterer at the mid-point of the array, a point scatterer at mid-point with beam pattern corresponding to 15-m vertical array, a number of point scatterers distributed over target depth, and a “volume flow” approach simulating scattering from a pressure release vertical cylinder. Results are compared with TREX13 measurements of the hose echo during a period at relatively low wind speed. [Work supported by US Office of Naval Research]*

Keywords: *waveguide, scattering, normal modes, target echo, finite cylinder, reverberation*

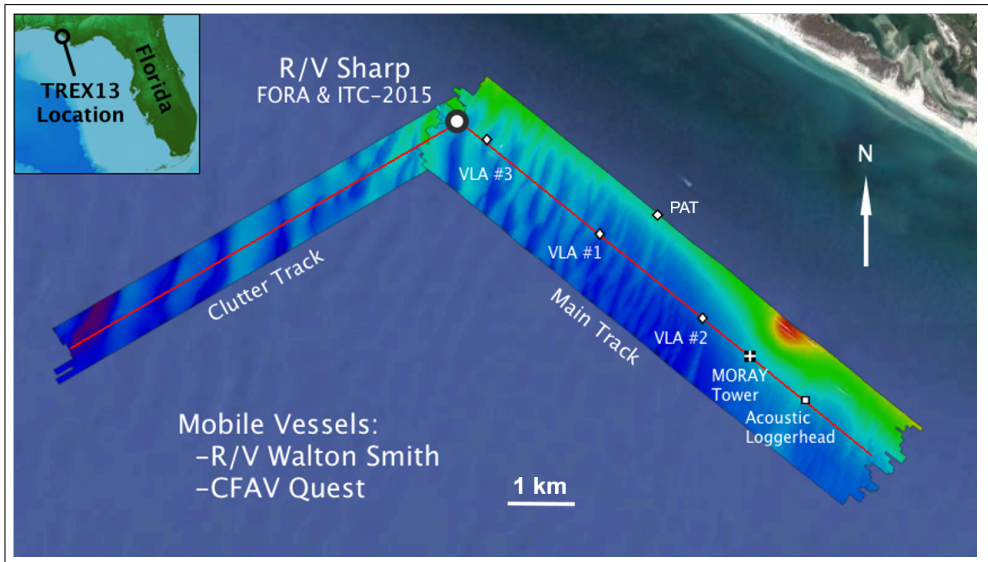


Figure 1: TREX13 site and locations of acoustic assets along the Main Track.

1. INTRODUCTION

The Target and Reverberation Experiment (TREX13) was conducted in shallow water in the Gulf of Mexico off Panama City, Florida, USA. Extensive acoustic measurements were made in April and May 2013 using pulses in various sub-bands between 1800 and 3600 Hz, generally with both source and receiver in fixed-fixed position. The unique feature of the experiment was a fixed source and fixed receiving arrays deployed in about 20 m of water. One of the main goals of the experiment was to obtain target echo, reverberation, and transmission loss measurements, over a month-long period, with an extensive set of companion environmental measurements before, during, and after the main experiment for prediction purposes. These measurements are to facilitate the understanding of the underlying reverberation and clutter mechanisms, and to support quantitative modelling. Previous results from various authors have been collected in a Special Issue in the IEEE Journal of Oceanic Engineering [1].

The objective of this work is to use normal modes to model the echo received from the air hose deployed during TREX13 and compare with field measurements. Figure 1 shows the TREX13 site and locations of acoustic assets. The ones of main interest here are the ITC-2015 source, FORA triplet line array deployed horizontally, and a vertical air-filled hose (labelled PAT).

2. MODELLING THE SCATTERED FIELD OF A CYLINDER IN A WAVEGUIDE

The most relevant reference for the scattered field was Kusel and Ratilal [2], which we denote here as KR09. However, it did not specify details for the levels or the normal mode approach, so we started with Ingenito [3], which gives in detail the equations for scattering from a sphere in an isospeed waveguide. We extended his formulation to scattering from a vertical cylinder using the work of Stanton [4], and added capability to handle a sound speed profile.

For constant sound speed, Stanton derived an expression¹ for the scattering of a plane wave

¹KR09 Eq. 14 differs by a factor of k/i .

incident on a cylinder of length L and radius a

$$S(\theta, \phi, \theta_1, \phi_1) = \frac{-iL \sin[(kL/2) \cos(\theta_1 - \theta)]}{\pi [(kL/2) \cos(\theta_1 - \theta)]} \sum_{m=0}^{\infty} B_m (-i)^m \cos(m[\phi - \phi_1]) \quad (1)$$

where $k = 2\pi f/c$ is the acoustic wavenumber in the water, θ and ϕ correspond to the elevation and azimuthal angles of the scattered plane waves, θ_1 and ϕ_1 correspond to the elevation and azimuthal angles of the incident plane waves, and

$$B_m = -\varepsilon_m i^m J_m(Ka) / H_m^{(1)}(Ka), \quad (2)$$

where J_m and $H_m^{(1)}$ are Bessel and Hankel functions, $\varepsilon_0 = 1$, and $\varepsilon_m = 2$ otherwise, and $K = k \sin \theta_1$.²

To get a measure of the absolute levels, we started with a “sonar equation” calculation, $EL = SL - TL1 - TL2 + TS$, where EL is the echo level, $TL1$ is the source-to-target transmission loss, $TL2$ is the target-to-receiver transmission loss, and TS is the target strength. For the target strength, the backscattering strength for a vertical cylinder at zero grazing angle $S(\pi/2, 0, \pi/2, \pi)$ is used. The echo level is then evaluated using transmission loss calculated by both the coherent and incoherent modal sums, the latter being smooth and monotonically decaying with range.

The next step is to use Ingenito’s formulation with the scattering function evaluated at the grazing angles of the modes at the center of the target. Ingenito’s equations are for a sphere, and for an environment with constant sound speed. However, equations for a non-spherical scatterer is given in his Eq. 51. Also, for a sound speed profile, his mode functions $u_n(z) = A_n \sin(\gamma_n z)$ can be generalized [5] to $u_n(z) = A_n(z) \sin(\psi(z))$. The normal-mode code used here contains a staircase of isospeed layers to approximate a sound speed profile; so within each layer the sound speed is constant. There is also the complication that for a target not at the minimum of the sound speed profile, some of the modes will be evanescent with imaginary incident angles. These were excluded from the calculations with the scattering function.

To confirm we had the correct levels, the Ingenito formulation was tested with an omnidirectional scattering function having the same TS as used in the sonar equation. It was found the Ingenito levels needed to be adjusted first by 4π (due to a unit source being $\exp(ikr)/(4\pi r)$), and by a factor of k ; the results then agreed exactly with the sonar equation. (For cases with the sound speed profiles, we included the evanescent modes in Ingenito’s formulation.)

One of the points from KR09 is that, with a sound speed profile, over the depth of the vertical array the mode angles will change, sometimes from imaginary to real. Thus, it is not really a plane wave that is incident on the array, and the pressure needs to be evaluated at each depth. For a vertical line array (VLA) of N_{el} elements the scattered field can be written as

$$P_{scat}^{VLA} = \sum_{t=1}^{N_{el}} \sum_{n=1}^N \sum_{n'=1}^N P_n^{ST}(z_t) P_{n'}^{TR}(z_t) E_{nn'}(z_t), \quad (3)$$

where N is the number of propagating modes, $P_n^{ST} = \sqrt{2\pi i} u_n(z_s) u_n(z_t) \exp(ik_n r - \delta_n r)/(k_n r)$ is the source-to-target propagation, and P_m^{TR} is the similar target-to-receiver propagation factor. As a first approximation, each element $E_{nn'}$ can be treated as omnidirectional, with scattering $1/N_{el}$ of the target strength amplitude used for the earlier “sonar equation” calculations. The

²The original equations in Stanton [4, Eq. 12] and KR09 [2, Eq. 15] use lowercase k , but Stanton notes it should be multiplied by the sine of the incident angle, and he explicitly shows it in his Eqs. 33–36. [The $\pm i^m$ in the two equations seem to cancel, so it is not clear why they are there.]

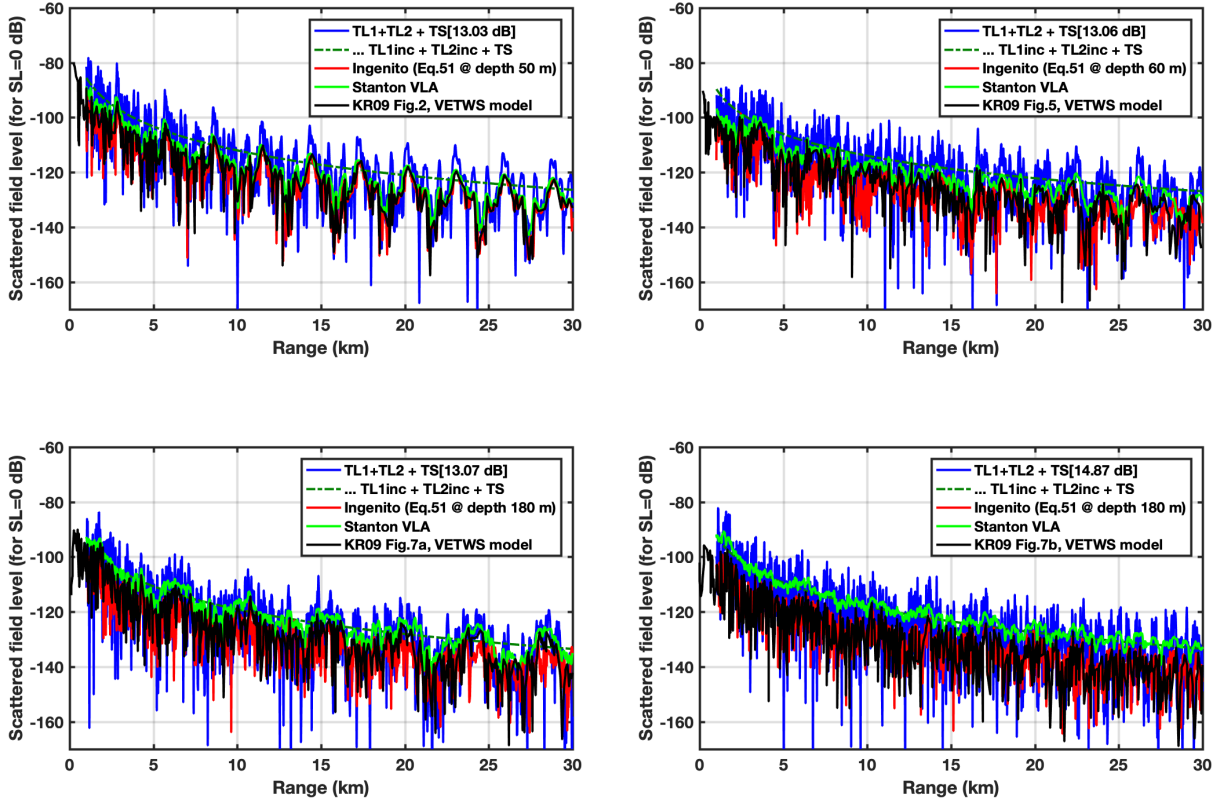


Figure 2: Various calculations of scattered field compared to KR09.

scattering strength is omni-directional with no phase dependence, but the scattering from the array elements is added coherently. The “volume flow” approach of Stanton improves on this. From Eq. (2), for backscatter $\phi = \pi$, so $\cos(m\phi) = (-1)^m$

$$E_{nn'} = -\frac{i}{\pi} \sum_{m=0}^{\infty} (-i)^m (-1)^m (-\varepsilon i^m) J_m(Ka) / H_m^{(1)}(Ka) = \frac{i}{\pi} \sum_{m=0}^{\infty} \varepsilon_m (-1)^m J_m(Ka) / H_m^{(1)}(Ka). \quad (4)$$

This depends on the incident vertical angle through K , and has a slight depth dependence, $k = (2\pi f)/c(z)$. With an isospeed environment, one would get the analytical sinc function of Eq. 1. The volume flow approach agrees quite well with a simple VLA approach with N_{el} omni-directional elements.

The comparison of various calculations of scattering field versus range, with the results of KR09 is shown in Fig. 2. A vertical air-filled cylinder of length 30 m and diameter 7 cm is modelled as pressure release target. This corresponds to the “BBN hose” described by Malme [6]. Since ka is small, in Eq. (1) the summation to $m = 2$ is sufficient; elements spaced every 1 m are used in this work. Four cases are shown:

- (1) upper left: a Pekeris environment at 415 Hz, in 100 m water with both source and receiver at 50 m, and target centered at 50 m depth;
- (2) upper right: a shallow water sound channel of 200 m water depth with minimum sound speed at ~ 92 m depth, source and receiver at 60 m, and target centered at 60 m, again at 415 Hz;
- (3) lower left: the same as case 2, except the target is centered at 180 m;
- (4) lower right: the same as case 3, except now at 950 Hz.

In each sub-plot there are five curves. The sonar equation is basically the two way transmission loss to a point target at some depth; the scattering is omni-directional. The calculation using the incoherently-summed modes gives a smooth range-averaged curve. The Ingenito approach

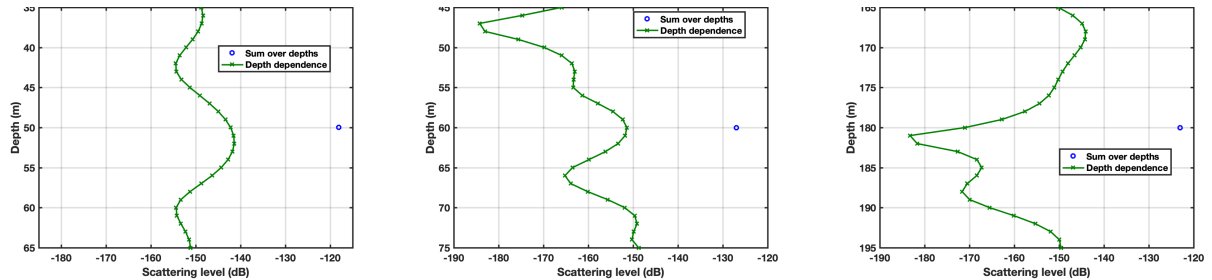


Figure 3: Scattered field versus depth at range 20 km corresponding to KR09 examples at 415 Hz.

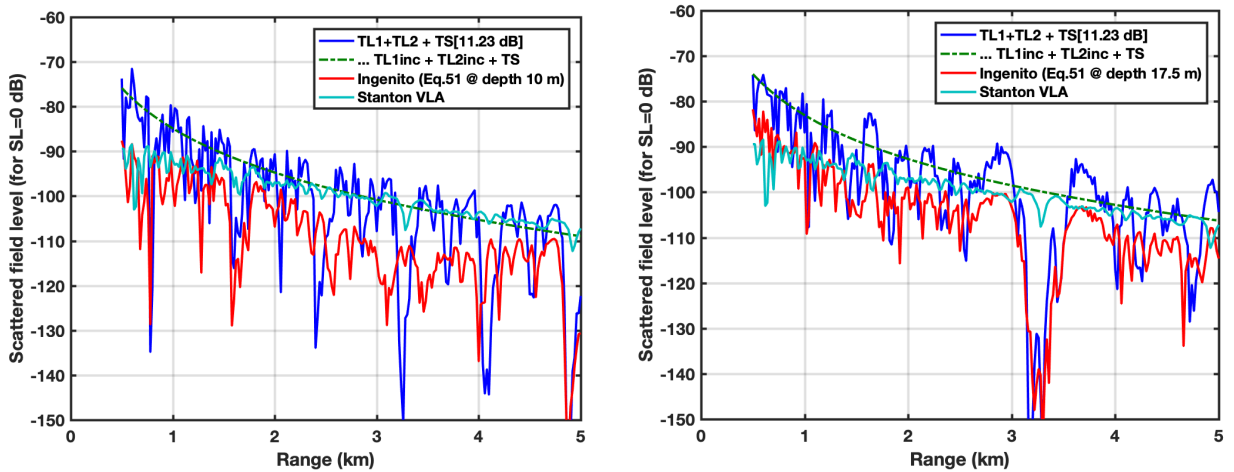


Figure 4: Scattered field versus range for TREX13 environment at 3150 Hz: (left) point target near 10 m depth; (right) point target near 17.5 m depth.

uses the scattering function at mid-depth of the vertical cylinder. Due to the beam pattern of the scattering function, the scattering is reduced at angles away from the incident angle. The Stanton VLA approach integrates over the length of the array, and therefore is much smoother. The KR09 results are overlaid in black; their calculations are also integrated over the depth of the array, but are more “spiky” than that of the Stanton approach.

Overall, our implementation of the Ingenito approach seems to give the best agreement with the KR09 results. (It is in better agreement than the figures shown in the KR09 paper; e.g., one should compare the lower-right panel with Fig. 7b of KR09.) The Stanton VLA approach is much smoother, and compares quite well with KR09 and Ingenito for the first 3 cases. However, it seems several dB higher for the 915 Hz example, but it is close to the simple incoherent sonar equation results.

Calculations of scattering strength versus depth at 20 km corresponding to the KR09 examples at 415 Hz are shown in Figure 3. Our agreement with KR09 is only marginal. The levels of this work are higher toward the sound channel, as one might expect, but there will be considerable variation with range.

An example from TREX13 at 3150 Hz is shown in Fig. 4. We use the TREX13 “Strawman” environment: the water is isospeed at 1525 m/s, of water depth 19.6 m, over a halfspace of relative density 1.9, sound speed 1660 m/s, and attenuation 0.5 dB/(m-kHz). The source and receiver are at 18.4 m and 17.5 m respectively, and the 15 m hose of diameter 7.5 cm spans depths from 2.6 m to 17.6 m. For illustrative calculations the target beam pattern is set at 10 m (left) and 17.5 m (right). For the sonar equation calculation, the target strength is for backscatter at zero-degree grazing angle. The VLA result using Stanton’s volume flow approach

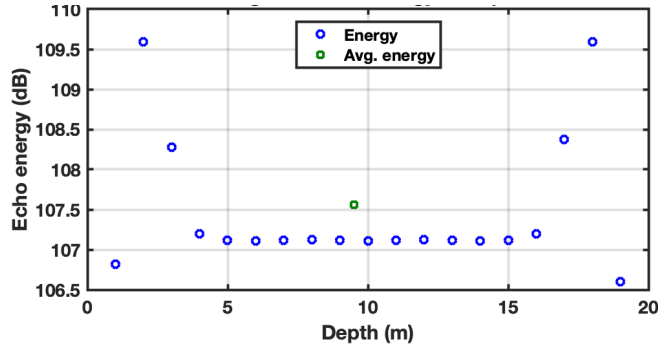


Figure 5: Calculated echo strength versus depth at 3150 Hz.

is coherently summed over 16 element depths. Note: the VLA calculation is the same in both plots; the range dependence of the coherent transmission loss is quite different at the two depths; there is slightly lower transmission loss to depth 17.5 m than to 10 m (see the incoherent curve), due to the source and receiver being close to the bottom; with the beam pattern at a single point the scattered field is quite different at the two depths. Figure 5 illustrates the range-averaged echo strength versus depth (see next section). Note how it is basically flat, except for a peak near the source/receiver depths and correspondingly near the surface; it drops again near the boundaries.

3. MODELLING TIME DEPENDENCE USING MODE GROUP VELOCITIES

The methods discussed in Section 2 use a single frequency, so the results are very sensitive to depth and range. Also there is only range dependence, and no time dependence. Therefore, to simulate the echo from a matched filtered LFM would require convolving with many frequencies.

As an interim measure, an energy-based formulation at a single frequency with modal group velocities is used to simulate the echo return. The reverberation formulation using modal group velocities [5] can be extended to handle the echo from a target [7, 8].

The echo time series from target at range r and depth z_T is given by [8]

$$T_e(t; r) = \left(\frac{2\pi}{\rho_s \rho_T r} \right)^2 \sum_{n=1}^N \sum_{m=1}^N \frac{[u_n(z_S)u_n(z_T)]^2 [u_m(z_R)u_m(z_T)]^2}{k_n k_m} \times \exp[2(\delta_n + \delta_m)r] e_{nm}(z_T) I_0(t - t_n - t_m). \quad (5)$$

All the angle-dependent echoes e_{nm} are from range r , but the arrival time of each mode pair is determined by the group velocities: $t_n = r/g_n$.

An alternate formulation, using up-and down-going waves, like reverberation, can be used, with the following replacements:

$$u_{n[m]}(z_T) \Rightarrow A_{n[m]}(z_T), \quad (6)$$

$$e_{nm} \Rightarrow E_{nm} = e_{n,m} + e_{n,-m} + e_{-m,n} + e_{-m,-n}.$$

The mode functions oscillate rapidly with depth, so the terms in Eq. (5) can vary rapidly with depth. The amplitudes $A_n(z_T)$, however, are like an envelope, always positive, and vary slowly with depth, so produce a smoother depth dependence suitable for an extended target.

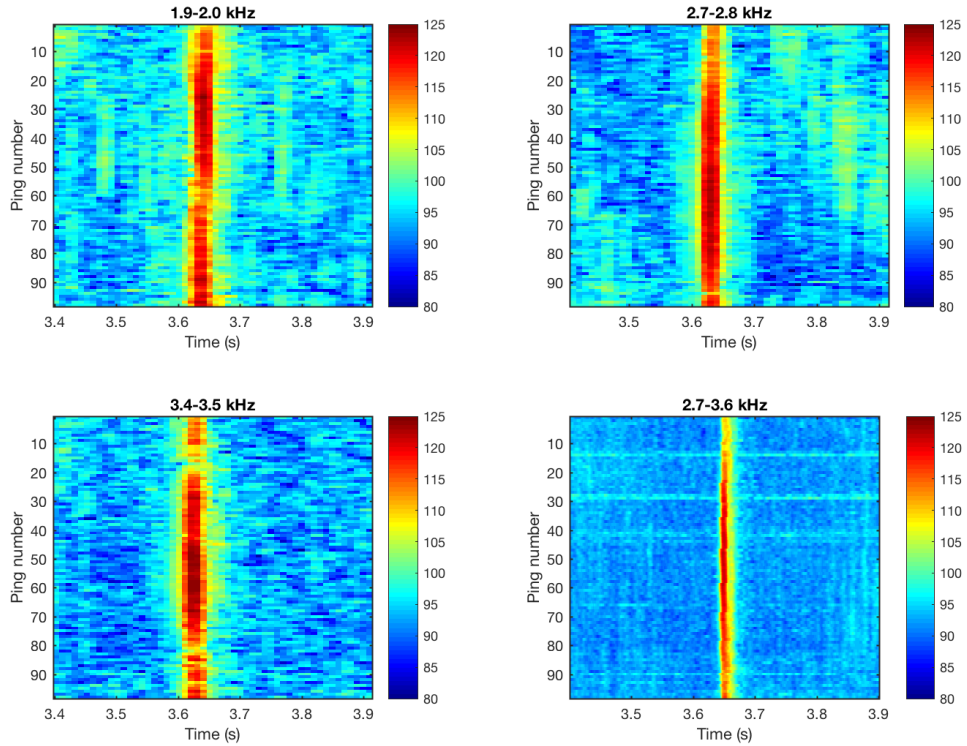


Figure 6: Echo from vertical hose received on FORA for four pulse types.

4. COMPARISON WITH LFM DATA

The echo returns from the vertical hose received on FORA for four LFM pulse types during overnight Run 79 (May 9, 2013, with 98 pings of each type) are shown in Fig. 6. The duration of the echo is on the order of 0.01 s for the 100 Hz bandwidth LFM, and 0.0011 s for the 900 Hz LFM. The received echo is stronger during the middle of the night, except for the 1.9–2.0 kHz LFM. Here we try a model comparison with the 900 Hz bandwidth data.

Figure 7 shows a calculation of reverberation and echo using the modal group velocity approach. The data are from a 2.7–3.6 kHz LFM from FORA beam of bearing 113°, which is steered towards the vertical hose. The model prediction uses the “Strawman” environment at 3150 Hz, with bottom scatter $\mu_3(\sin \theta_m \sin \theta_n)^{3/2}$, with $10 \log_{10} \mu_3 = -20$ dB. (For illustrative purposes, the bottom scattering is enhanced by 10 dB for an annulus of 20 m range extent near time 3.3 s.) This “ $\sin^3 \theta$ ” backscatter fits the fall off of the reverberation relatively well. The reverberation prediction is for a cylindrically symmetric environment, so has been reduced by 20 dB corresponding to the reverberation response of the beam [8]. The beam response should be unity in the direction of the vertical hose, so the echo prediction is not reduced. Note how the modal group velocity introduces time spreading [9], reducing the peak about 10 dB compared to a simple sonar equation approach (right plot, cyan curve). (It is worth noting that level of –100 dB for “Stanton VLA” at 3.65 s in Fig. 4 combined with using source energy 193.8 dB, pulse compression of 29.5 dB, spreading loss of 10 dB, and target strength of 4 dB, gives 117.3 dB, consistent with the value shown here for no time spreading.) The target strength here is modelled as 4 dB, which seems too low. The Stanton backscattering strength is about 11 dB, and other estimates from TREX13 have been the order of 10 dB. Also, the data shown are from a single ping, and the echo data in Fig. 6 vary over the course of the night. The predictions are in a reasonable range, but clearly more scrutiny is needed in future work.

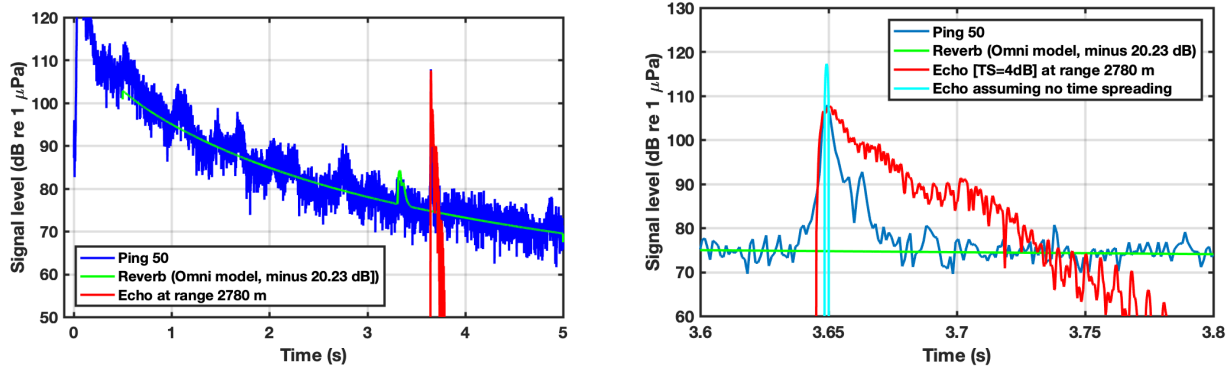


Figure 7: Left: Data from 2.7–3.6 kHz LFM for FORA beam on bearing 113°, along with model prediction of reverberation and target echo. Right: Enlargement of echo region, with additional curve (in cyan) illustrating the effect of no time spreading.

5. CONCLUDING REMARKS

Our initial attempt to model the echo from a vertical air-filled hose is presented here as a pressure release target. Various models are used to calculate the coherent scattered field at a single frequency, and compared with published results. Using the sonar equation as a reference, reasonable comparisons with KR09 are achieved.

For now, as an interim measure, a modal group velocity approach to obtain a measure of the time spreading of the target echo is adopted. This only requires a calculation at a single frequency, though, for large bandwidths, averaging over a small number of frequencies would be better. To compare with field data, the pulse-compressedLFMs, time dependence is needed, which would require combining the results over many frequencies with the source spectrum. This work is currently ongoing, and anticipated to require significant computation.

REFERENCES

- [1] B. T. Hefner and D. Tang. Guest editorial: Target and Reverberation Experiment 2013 (TREX13)—Part I. *IEEE J. Oceanic Eng.*, 42(2):247–249, 2017. Also, *ibid.*, ... —Part II. 42(4):757–758.
- [2] E. T. Kusel and P. Ratilal. Effects of incident field refraction on scattered field from vertically extended cylindrical targets in range-dependent ocean waveguides. *J. Acoust. Soc. Am.*, 124:1930–1936, 2009.
- [3] F. Ingenito. Scattering from an object in a stratified medium. *J. Acoust. Soc. Am.*, 82:2051–2059, 1987.
- [4] T. K. Stanton. Sound scattering by cylinders of finite length. *J. Acoust. Soc. Am.*, 83:55–63, 1988.
- [5] D. D. Ellis. A shallow-water normal-mode reverberation model. *J. Acoust. Soc. Am.*, 97:2804–2814, 1995.
- [6] C. I. Malme. Development of a high target strength passive acoustic reflector for low-frequency sonar applications. *IEEE J. Oceanic Eng.*, 19:438–448, 1994.
- [7] D. D. Ellis, T. J. Deveau, and J. A. Theriault. Volume reverberation and target echo calculations using normal modes. In *Oceans '97 MTS/IEEE Conference Proceedings*, Vol. 1:608–611, Halifax, NS, Canada, Oct. 1997.
- [8] D. D. Ellis, J. Yang, J. R. Preston, S. Pecknold. A normal mode reverberation and target echo model to interpret towed array data in the Target and Reverberation Experiments. *IEEE J. Oceanic Eng.*, 42:344–361, 2017.
- [9] M. A. Ainslie and D. D. Ellis. Echo, reverberation, and echo-to-reverberation ratio for a short pulse in a range-dependent Pekeris waveguide. *IEEE J. Oceanic Eng.*, 42:362–372, 2017.